ELSEVIER

Sensors and Actuators A 45 (1994) 227–236

SENSORS AND ACTUATORS A PHYSICAL

Assembling three-dimensional microstructures using gold–silicon eutectic bonding

A.-L. Tiensuu, M. Bexell, J.-Å. Schweitz, L. Smith, S. Johansson

Department of Technology, Uppsala University, Box 534, S-751 21 Uppsala, Sweden

Received 28 December 1993; in revised form 15 July 1994; accepted 19 August 1994

Abstract

An assembly method for three-dimensional microelements is presented. The assembly is done in situ with a micromanipulator in an SEM using Au–Si eutectic bonding. Microblocks bonded to larger silicon substrates are used for evaluation of the mechanical strength and a microarch is presented to demonstrate the possibilities of the technique. The microelements are fabricated by bulk micromachining, and sputter deposited with chromium and gold. Etched (111) faces have been successfully bonded. TEM investigation of samples from vacuum furnace experiments show large gold grains with smaller chromium silicide grains in the bonded region. The silicon in the eutectic liquid precipitates epitaxially on both silicon faces. Mechanical bending tests on the microblocks give sufficiently high fracture stresses for the intended applications in microrobotic systems. Average fracture stresses of 65 MPa are measured for one set of parameters. Problems encountered are misalignments of the microelements during processing and void formation in the bonds. It is believed this is connected to the experimental equipment and set-up. The microarch, which consists of three assembled microblocks, reaches a tensile stress of 16 MPa, encouraging further development. In conclusion, strong microbonds are achieved using a solidified gold–silicon eutectic melt as an adhesive, and it is demonstrated for the first time that three-dimensional microassembly by means of eutectic bonding of micromachined elements can be performed by manipulation and processing on a locally heated specimen table.

Keywords: Eutectic bonding; Gold; Microstructures; Silicon

1. Introduction

The growing interest in complex microsystems has resulted in considerable research efforts even within microfabrication techniques not directly intended for batch processing. One such research field is assembling microcomponents into larger systems. If we consider a complex microsystem including sensors, actuators, mechanical details, etc., we would like to have a general assembly method for all types of components. This article will address this problem and in particular that of building three-dimensional microstructures of micromachined silicon elements. Expected problems are concerned with the bond quality for various microcomponents and the positioning equipment. It should be possible to assemble three-dimensional structures arbitrarily, hence an advanced micromanipulating equipment compatible with the processing is desirable. Various types of equipment for the manipulation of microelements are presently being developed [1–3] and the unit developed for our experiments operates in situ in a scanning electron microscope (SEM).

Different bonding techniques are already used in the microelectronics industry and the main application areas are sealing, die attachment and electrical interconnects. A variety of bonding/sealing techniques, such as silicon fusion bonding [4–6], anodic bonding [7,8], low-temperature-melting glass [9,10] and eutectic bonding [11], capable of creating strong bonds has been presented and explored during the last decades. In the case of building a complex microsystem, the bonding should be generally applicable, e.g., have the ability of joining different materials with various surface conditions. Furthermore, if the different components in the microsystem should be able to communicate, an electrically conductive bond is advantageous. Eutectic Au–Si bonding is a technique that possesses the above-mentioned features and also has potential for three-dimensional assembly. It also has attractive features, such as a low processing temperature and liquid-phase bonding. One problem encountered in conventional Au–Si eutectic

SSDI 0924-4247(94)00836-7

bonding is the presence and formation of surface oxides inhibiting the bonding [12]. These effects are to some extent avoided in our experiments, which are performed in vacuum.

The aim of this work is to demonstrate the possibility of three-dimensional assembly of silicon microelements using Au–Si eutectic bonding. In all cases, both Si surfaces to be joined were coated with a thin Au layer. A basic microelement was manufactured, with two etched sides and two polished sides prepared for bonding. Using these elements, a three-dimensional structure was assembled. To evaluate the bond strength between an etched side of an element and a polished silicon surface, several samples were made by bonding a microelement to a polished substrate. Little attention has previously been paid to the bonding properties of etched surfaces. In the assembly of micromachined elements, however, the problem of joining etched surfaces by bonding becomes essential. Bonding and testing of the bond strength were performed in a micromanipulator developed at Uppsala University.

2. Experimental

2.1. Macrobonding experiments

A preliminary bonding study was performed in order to determine suitable process parameters, such as the bonding temperature and the need for a thin intermediate chromium layer under the gold film for improved adhesion and as a diffusion barrier [12]. The bonding tests were carried out at three different temperatures in a top-and-bottom heated vacuum furnace at a pressure of $(4–5)\times10^{-6}$ torr. In this experiment (111)-type polished silicon was used. It was cut into 5 mm × 10 mm and 10 mm × 10 mm pieces, cleaned, and sputter deposited at a base pressure of $(1–2)\times10^{-6}$ torr with an Ar pressure of 9 mtorr. The total film thickness was measured over a surface step with a surface profilometer. After sputter deposition, the samples were rinsed in isopropanol and dried with filtered N_2 in order to remove dust or other particles. The samples were put together in pairs (one bigger and one smaller), placed in the vacuum furnace, clamped by a small spring force and annealed according to Table 1. Simple strength tests like breaking the samples or trying to separate a bonded couple by forcing a sharp wedge into the bond were performed. The free surfaces of the samples were examined in an SEM.

A first investigation of the internal structure of the bond was done by polishing an oblique cross section from a successfully bonded sample. A dimple grinder was used in order to get a wide transition region from the upper silicon plate, through the bond and down into the lower/bottom silicon plate. The final polishing step was done with a soft cloth and 0.25 μm diamond particles. Fig. 1 shows the geometry of the specimen prepared with the dimple grinder. This sample was then examined in the SEM.

A sample from the same bonding study was also analysed in a transmission electron microscope (TEM, JEOL 2000 FX II). Cross-sectional TEM samples were prepared as follows. Additional bulk silicon was glued to both sides of the bonded specimens with epoxy. Curing of the epoxy bond was carried out at 160 °C for 4 h. A cross section through this sandwich was cut and ground mechanically to a thickness of about 100 μm. Mechanical thinning and polishing were carried out with a dimple grinder to a thickness of about 5

Table 1
Process steps of the macrobonding and microbonding experiments

Process step	Macrobonding experiments (furnace annealing)	Microbonding (heating plate)	
		Substrate	Microelement
1. Photoresist coverage	yes	yes	yes
2. Dicing	yes	yes	no
3. Micromachining [a]	no	no	yes
4. Cleaning step [b]	yes	yes	yes
5. Cr film thickness (nm)	5–10, none	5–10	5–10
6. Au film thickness (nm)	150	100, 240	200
7. Photoresist coverage	no	no	yes
8. Dicing	no	no	yes
9. Cleaning step [c]	no	no	yes
10. Bonding temperature (°C) (time = 10 min)	375, 455, 520	510–520	

[a] KOH etching in 29% solution at 80 °C.

[b] 10 min in boiling RCA1 (5:1:1, H_2O:NH_3:H_2O_2) an boiling RCA2 (6:1:1, H_2O:HCl:H_2O_2), rinsing in distilled deionized water and HF dip (1:50–100, HF:H_2O).

[c] Three rinses in acetone in an ultrasonic bath and rinsing for a few minutes in warm RCA1.

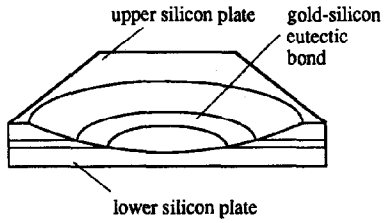

Fig. 1. Schematic drawing showing the geometry of the specimen prepared with the dimple grinder.

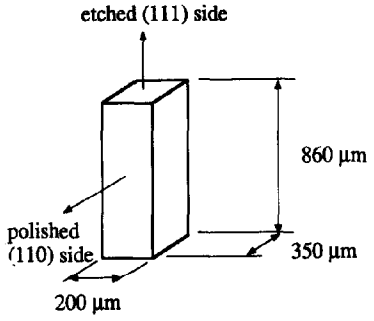

Fig. 2. Crystallographic orientation and geometry of the microblock.

μm. Final thinning to electron transparency was done by argon-ion milling at low acceleration voltage (3 kV) and at a low angle of incidence (12°) of the ion beam to reduce the heating of the sample and ion-beam-induced artefacts.

2.2. *Fabrication and bonding of microelements*

The microsized elements used in the assembly experiments were made from (110)-type double-polished silicon wafers. First, 0.9 mm wide beams were made by etching rectangular grooves through the wafer [13,14]. Parallel (111) planes, perpendicular to the original polished (110) plane, constituted two sides of the beam. The etching was done using 29% KOH at a temperature of 80 °C. After etching, the beam was cleaned in the same way as the samples in the macrobonding experiments and then mounted on a rotating holder inserted in the sputter chamber. This was done to achieve a four-sided deposition in order to have microblocks with four sides available for three-dimensional building. The sputtering parameters were the same as mentioned earlier. The surface smoothness was measured, before deposition, on the etched side of the beam using a surface profilometer. After sputter deposition the beam was cut into microblocks using a dice saw. To protect the deposited surfaces during cutting, the beam was covered with photoresist. The final dimensions of the microblocks were approximately 860 μm × 200 μm × 350 μm. Fig. 2 illustrates the geometry and crystallographic orientation of a microblock.

The substrate material used in the assembly experiments was (111)-type silicon prepared in the same way as in the macrobonding experiments. Two different gold film thicknesses were used in two bonding series (see Table 1).

Eutectic bonding of microsized elements was performed in a micromanipulator in situ in an SEM [3]. The main parts of the manipulator are a heating unit and a pair of tweezers used together with a supporting probe. The probe and the tweezers are located on two motorized tables that can be moved in the *x*-, *y*- and *z*-directions, independently of each other. The tweezers may be rotated ±90° around their longitudinal axis. The heating unit is mounted on a table movable in the *x*- and *y*-directions. The temperature is measured by a thermocouple inserted into a horizontal hole in the heating plate. The heating table and the tweezers are shown in Fig. 3. One example of a positioning experiment is shown in Fig. 4. Here a microelement, different from the ones used in these bonding experiments, is positioned in a micromachined V-groove on a substrate. The microelement can be inspected by rotation of the tweezers. At the front end of the heating unit there is a horizontal cold table where the microelements are temporarily placed before the manipulator is inserted into the SEM. A substrate plate is clamped to the heating table and one of the microblocks is picked up with the tweezers and positioned with one of its etched deposited sides on the substrate plate. The microblock is then clamped with the supporting probe during the bonding. Microblocks bonded in this way were used for evaluation of the bond strength.

The assembly procedure of the structure containing three microblocks was carried out slightly differently from the single microblock bonding. First one microblock is positioned as described earlier and the second one is placed beside it using the tweezers (Fig. 5). These

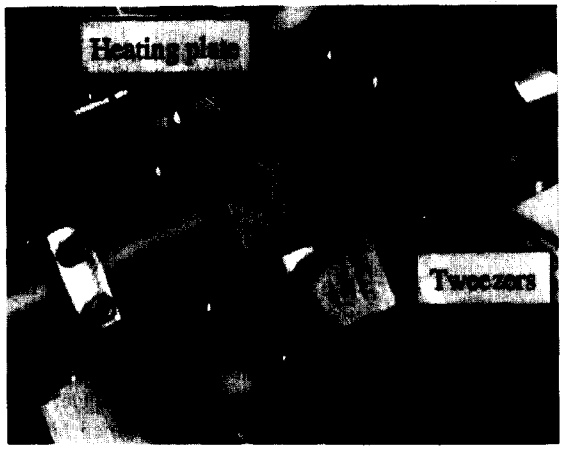

Fig. 3. The heating unit (centre) and the tweezers (right) in the micromanipulator.

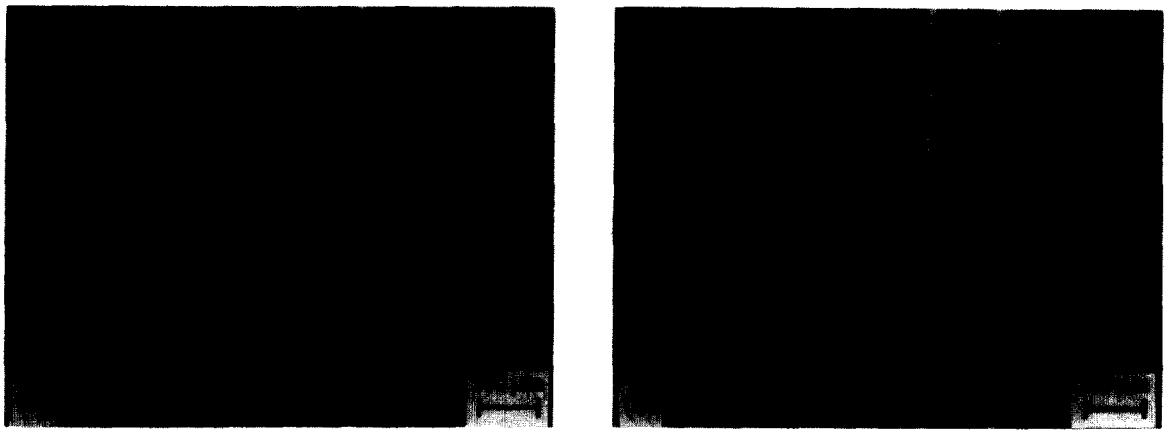

Fig. 4. (a) Positioning of a microelement in situ in an SEM. (b) The element is turned using the tweezers.

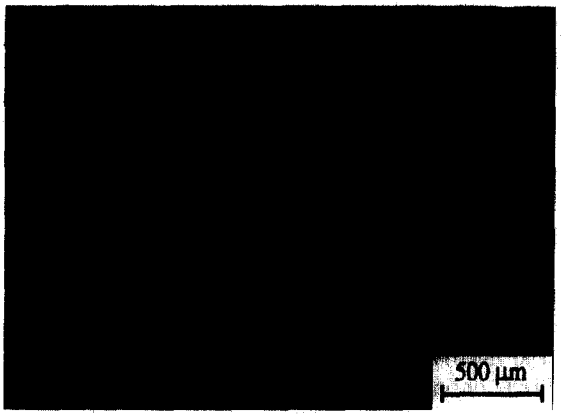

Fig. 5. Placing of the supporting microblocks in the assembly of the three-dimensional structure in situ in an SEM.

Fig. 6. Bonding of the third microblock in the three-dimensional structure in situ in an SEM.

are the supporting microblocks in the structure and they are heated to ≈420 °C. They are kept at this temperature for a few minutes and then cooled down to <200 °C. This heat treatment is enough to make them adhere to the substrate and both the supporting probe and the tweezers can be removed. Then the third microblock is placed with one of its polished sides on top of the etched upper surfaces of the other microblocks and the entire structure is clamped and heated to ≈520 °C where it is held for 10 min (Fig. 6).

2.3. Evaluation of the microbonds

The bond strength of the single-bonded etched microblocks was measured by applying a horizontal force at the upper end of the standing microblock and registering the fracture limit. The force was applied by means of a tungsten rod bent into a 90° angle, and the sample was mounted in a special specimen holder with force cells for lateral measurements. The tungsten rod and the specimen holder were mounted in the micromanipulator. The motorized stages were used for positioning the rod and for applying the force. The maximum tensile stress is given by

$$\sigma_{z,\max} = \frac{M_{y,f}}{I_y / x_{\max}} \tag{1}$$

where $M_{y,f}$ is the bending moment at fracture, I_y is the moment of inertia when a force is applied to the microblock in the x-direction and $x_{\max} = h/2$, as shown in Fig. 7. After fracture testing of the single-bonded microblocks, surface profilometry was performed to determine the final bond thickness.

A separate tensile test was performed in the micromanipulator to measure the bond strength of the assembled three-dimensional structure. A nylon thread of 0.14 mm diameter was inserted between the supporting microblocks and tied in a loop around the upper microblock. A probe for measuring force in the

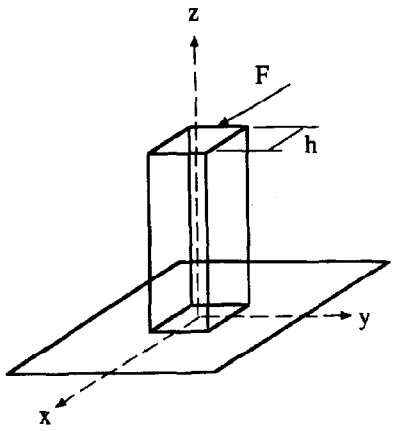

Fig. 7. Geometry of the bond-strength testing of the single-bonded microblocks.

z-direction was inserted in the loop. The force was applied by moving the probe in the z-direction with a motorized stage. In this way all bonded areas were loaded simultaneously.

To investigate the distribution of silicon precipitates in the bonded area, the gold was removed from the fracture surfaces by selective etching using aqua regia. A 1:2 mixture of HNO_3:HCl was used, and the samples were etched for 4 min in this solution at 60 °C. The fracture surfaces were investigated in the SEM before and after the etching.

3. Results

3.1. Macrobonding experiments

Samples from the macrobonding experiments were first evaluated by simple mechanical testing to find out if large non-bonded areas existed. In order to simplify the discussion, three different criteria are introduced here to classify the bonding quality in these tests. If the sample could be separated and there were signs of bonding at some, or few, points, it was considered *locally bonded*. Samples from the bonding at 455 and 520 °C with Cr and Au layers could not be separated by a wedge anywhere along the edge of the bonded silicon plates. These were regarded as *completely bonded*. If some pieces along the edge broke off the samples were considered *partially bonded*. The results of these experiments are displayed in Table 2. The coated surfaces outside the bonded region were investigated by the SEM, and the overall surface reaction appeared more homogeneous on the samples bonded at 520 °C. Based on these observations, Cr+Au films and a bonding temperature of 520 °C were chosen for the microbonding experiments.

Table 2
Results of the macrobonding experiments

Temperature (°C)	Deposited material	
	Au (150 nm)	Cr+Au (≈5+150 nm)
375	partially bonded	locally bonded
455	partially bonded	completely bonded
520	partially bonded	completely bonded

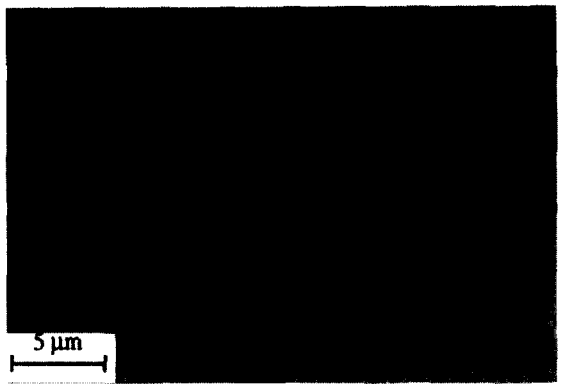

Fig. 8. SEM image of the specimen prepared with the dimple grinder.

The sample polished in the dimple grinder was investigated in the SEM. Fig. 8 shows the bond micromorphology in a 'semi lateral' view (oblique section) resulting from this type of preparation. Silicon ($Z=14$) is partially transparent to incident (and backscattered) electrons of 20 kV in comparison with gold ($Z=79$). The gold regions give higher intensity and appear as bright areas in Fig. 8. Darker areas with a size of about 1 μm are visible through the transparent silicon. Most of these are voids, as can be seen in the joint region. Possibly, some dark areas in the lower part of the joint are large silicide grains. The irregular shape of the Au region, seen in Fig. 8, is caused by a rough interface between the Au grains and the silicon matrix.

Investigations of the TEM specimens revealed several interesting phenomena. The interfaces between the joint and the silicon substrates were fairly rough, as was also seen in the oblique section of Fig. 8, indicating that reactions have taken place all over the surfaces. Along the joints investigated (about 50 μm in length) no sign of silicon grains or bridging could be found. Strain contrast, interpreted as small precipitates, was found in the silicon matrix. Mostly these precipitates appeared along a line parallel to the joint, indicating epitaxial silicon regrowth on the silicon substrate. These precipitates, ≈1–10 nm in size, could not be identified. The joint consists of large gold grains with sizes ≈10 μm, and other evenly distributed smaller grains (Figs. 9–10). These smaller grains have been identified as $CrSi_2$ by convergent beam electron diffraction, Fig. 9.

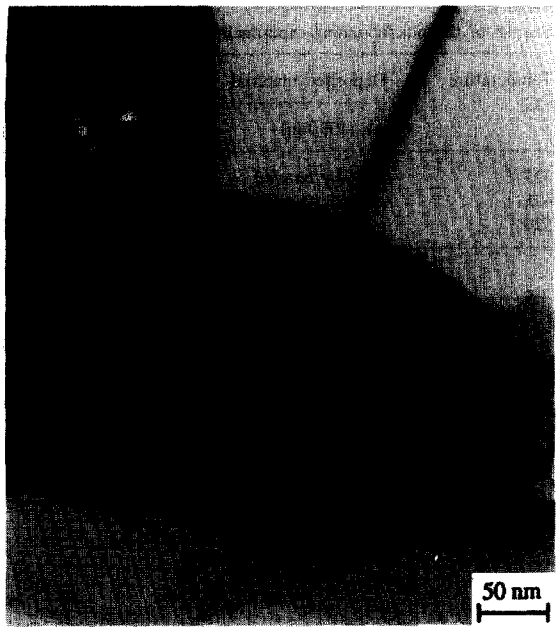

Fig. 9. Cross-sectional TEM image of vacuum furnace sample. The pointer indicates a $CrSi_2$ grain. Insert: corresponding convergent-beam diffraction pattern.

Both the gold and the silicide grains have grown more or less aligned to the silicon matrix, as was previously observed [15,16]. The silicon samples on each side of the joint were oriented similarly (a few degrees error). A high density of small strain contrast was seen in the Au grains, Fig. 10(a) and (b). These were too small ($\approx$1–5 nm) to be identified. Possible interpretations are small voids or small precipitates. A few voids of size $\approx$0.5–1 μm could be found in the bond of the TEM specimens, but some of these might have been preparation artefacts.

3.2. Fabrication and bonding of etched microelements

Surface profilometry, before deposition on the silicon beam, showed that the etched (111) side had an overall surface flatness typically of about 0.2 μm and no surface steps exceeding 0.5–0.6 μm over a 200 μm range. Before bonding of samples VI–XI, the etched and deposited surfaces of the microblocks were investigated in the SEM. Some defects were observed, e.g., saw dust attached to the gold film and detached film along the sides, etc. No clear relationship between the observed defects and the resulting bond strength was found.

When the microblocks were bonded, it was observed during annealing that the metal film 'disappeared' from a wide (typically 50 μm) region of the substrate surface around the microblock. It was also observed during cooling that a microblock began to change its position when the temperature passed approximately 480–490 °C. This happened although the microblock was mechanically clamped by a probe. One sample was seen to tilt sideways as one bottom edge of the microblock was raised about 5 μm relative to the substrate surface, i.e., the bond cross section became wedge shaped. The final microbond thickness was very high; typically ranging from 3 to 5 μm.

3.3. Evaluation of the microbonds

The results of the bond-strength testing of the single-bonded microblocks are compiled in Table 3. The results are also displayed as Gaussian distribution functions for samples I–XI and VI–XI, respectively, in Fig. 11. In the cases of thin substrate coatings (100 nm) no or rather weak bonding was obtained. For thicker substrate

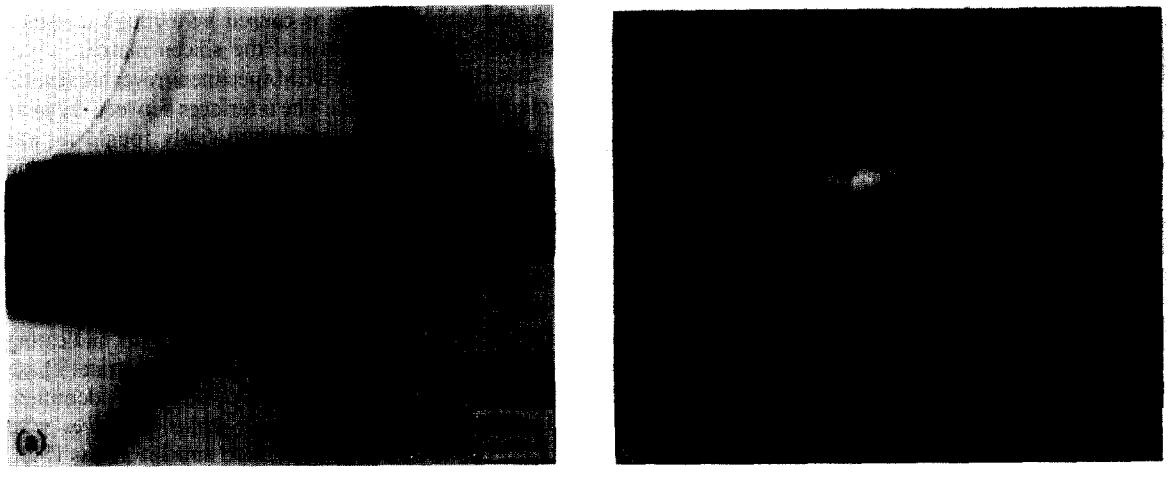

Fig. 10. Cross-sectional TEM image of vacuum furnace sample: (a) bright-field and (b) dark-field images of a large gold grain. An unusually large silicide grain is seen at the centre.

Table 3
Results of the bond-strength test of the single-bonded microblocks. Substrate gold-film thicknesses are 100 nm for samples I–V and 240 nm for samples VI–XI

Sample	Fracture stress σ (MPa)
I	
II	60
III	11
IV	31
V	
VI	93
VII	76
VIII	50
IX	26
X	46
XI	99

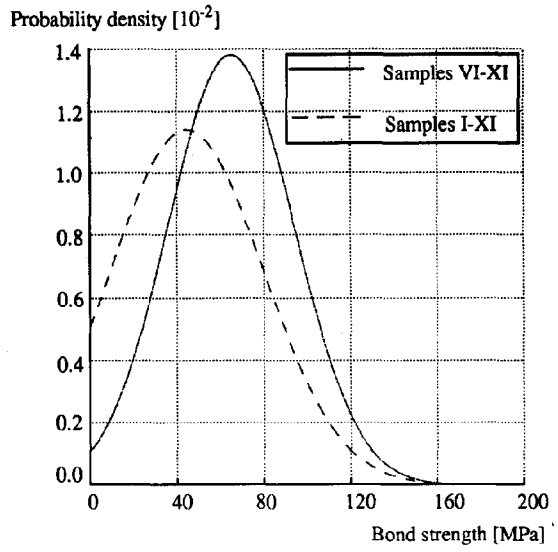

Fig. 11. Gaussian distribution functions of the results from the bond-strength testing of the single-bonded microblocks. Samples I–XI have a mean value of 45 MPa and a standard deviation of 35 MPa. Samples VI–XI have a mean value of 65 MPa and a standard deviation of 29 MPa.

coatings (240 nm) fairly strong bonding was obtained. Fracture occurred in the interface between the gold film and the bonded microblock. The bonds were not solid, but contained numerous voids of varying sizes and shapes. The microblocks showed patches of gold matching the shape of the voids in the bond. The patches did not 'fill in' the voids but were just the 'lids' on top of them. This is seen on the fracture surfaces after the bend-strength testing of sample VII in Fig. 12(a) and (b). The fracture seems to have propagated along the interface according to Fig. 13. Hence the crack has followed the Si–eutectic interface, but found it energetically more favourable to turn down into the voids close to the interface. In the voids of Fig. 12(a) small grains were seen at the bottoms. X-ray analysis (EDS) of these grains in the SEM resulted in a clear Cr peak.

Fig. 14 shows a free-standing three-dimensional structure, assembled according to the procedure described in Section 2. The microblock on top was bonded on two microblocks that had already been heated once to 420 °C. The visible misalignments in the structure are mainly due to the assembly procedure. The bond strength of the assembled three-dimensional structure was measured to be 16 MPa. It was the bonds of the upper (cross-beam) microblock that broke in the tensile test. The fracture surface showed an appearance similar to those of the single-bonded microblocks. Similarly to the single-bonded microblocks, the fracture occurred in the upper interface, but this time in an interface involving a polished Si surface.

Etching of the fractured surfaces of the single-bonded microblocks in aqua regia removed the gold from the bond and revealed the silicon microstructure. Fig. 15 shows the appearance of such an etched surface. The large faceted structures observed in the microbonds are 25–50 μm in size (e.g., the dark hexagonal area in Fig. 12(a)), extending from the substrate surface up to the microblock, and are most probably epitaxially grown from the substrate. Also the rest of the microstructure bridges the distance between the substrate surface and the microblock. A thin membrane has formed on top of the microstructure, maybe as part of the plate-like microstructure. The membrane has grown laterally along the interface between the solidified eutectic and the microblock. Surface steps on the microblock surface have been exactly replicated on the membrane, indicating that the membrane has grown in close contact with the microblock.

4. Discussion and conclusions

Assembling microelements into a complicated microsystem puts certain demands on the process. Some unexpected phenomena, which might cause problems in some applications, were observed during the experiments. The joint changed from an initial total film thickness of 240+200 nm to several micrometers and in some cases became wedge shaped. This might be critical for certain microsystem designs, particularly if sub-micron precision is desired. The exact mechanism for these misalignments remains to be investigated. One important factor that is difficult to avoid is relative movement due to thermal expansion of the heating unit. The temperature difference during annealing would create displacements in the manipulator of the order of tens of micrometers in the most unfavourable cases.

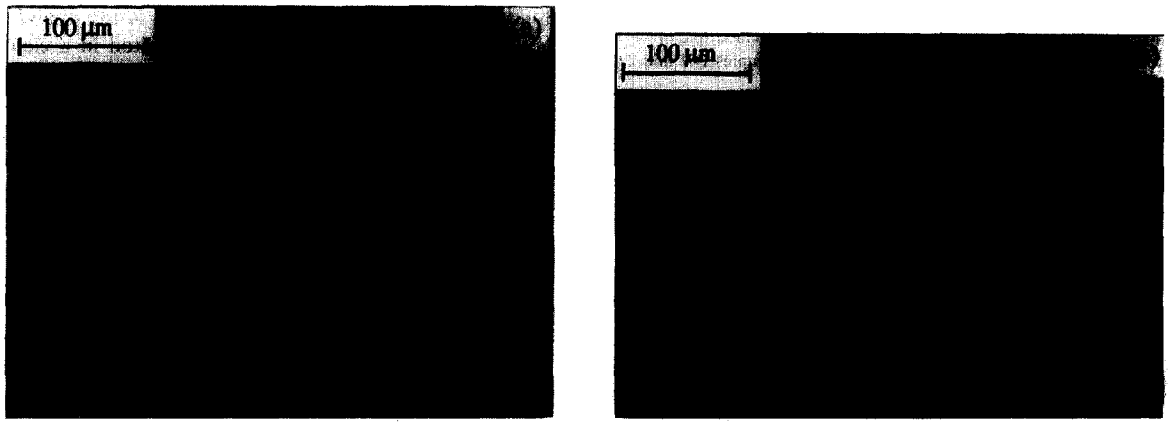

Fig. 12. SEM images of the fracture surfaces of sample VII, showing (a) voids in the remaining gold–silicon bond on the substrate and (b) the matching gold film patches on the microblock surface. Note the large silicon precipitate shown as the large hexagonal area.

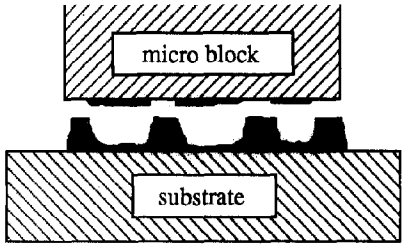

Fig. 13. Schematic cross-sectional view showing how the fracture has propagated through the bond.

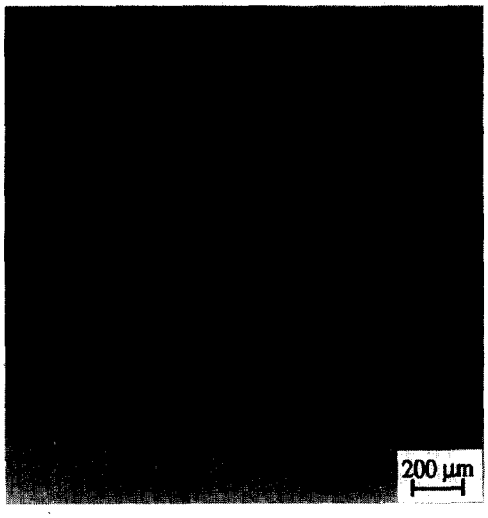

Fig. 14. The assembled three-dimensional structure.

No bond expansion could be measured in the furnace-annealed samples from the macrobonding experiments. The accuracy of these measurements was no better than about 10%, since it was difficult to determine the average interface spacing and the amount of silicide. Few and small voids were observed in the SEM and

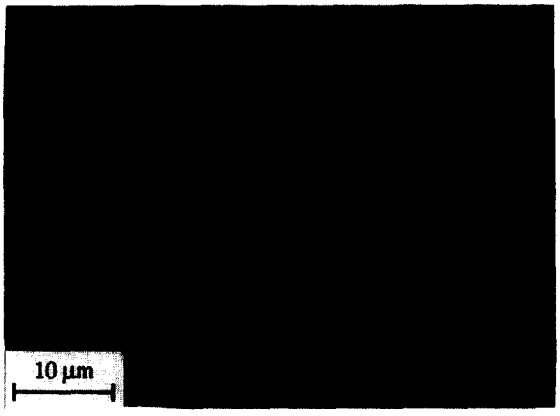

Fig. 15. After strength testing of the microbonds, the fracture surface of the substrate was selectively etched with aqua regia to remove the gold. This SEM image shows the remaining silicon structure in the bond.

TEM investigations. The main mechanism to compensate for an increased vertical distance in the furnace experiments would be void formation. Two important differences between the microassembly and the furnace experiments are the geometry of the samples and the thermal gradients during solidification. Inspection of the fractured bonds from the microbonding experiments revealed a large number of big voids and an intricate microstructure of silicon in the gold matrix. Void formation is usually ascribed to poor wetting of the eutectic melt due to surface oxides or surface contaminants [12,17]. In our case, however, this explanation is less likely. Close inspection of the voids in fractured bonds shows a contact angle between the solidified gold and the substrate that indicates good wetting. This is further supported by the oriented growth of the gold grains relative to the silicon substrate, as observed in the TEM investigations.

Understanding of the morphological changes during bonding is important for optimization of technological parameters such as strength and alignment. At a bonding temperature of 510–520 °C, approximately 25 at.% silicon is dissolved into the eutectic melt according to the Au–Si phase diagram [18]. In accordance with Ref. [19], the precipitation of Si will occur by epitaxial growth on either of the silicon surfaces, the substrate or the microblock. The growth rate of a crystal increases with temperature, hence the epitaxial regrowth on the warmer side should be the dominant process. The thermal gradient from the substrate surface up to the microblock gives an unstable solidification front, which promotes growth of the silicon structures in the same direction as the thermal flow. According to Ref. [20] the micromorphology of a particular system changes with the thermal gradients in the liquid in combination with the growth rate of the discontinuous phase. A comparison with work on the Al–Si eutectic system cited in Ref. [20] shows that various microstructures of silicon form that correspond well to the microstructures observed in our bond. These microstructures range from large faceted structures to faceted rods and various plate-like morphologies.

Fracture is probably initiated at an unbonded area close to the edge or at a void. It appears that the crack runs between the 'original' microblock surface and the top of the solidified structure. In one of the strongest bonded specimens, the fracture actually occurred in the silicon on the microblock side of the bond. This indicates that Au–Si adhesion of the same strength as that of the substrate side can also be obtained on the the upper side. An alternative explanation would be formation of strong silicon bridges. One effect that limits crack propagation along the interface on the lower side is the irregular interface morphology. The strength of the bonded structures is largely decreased by the unbonded areas along the edges and to a minor extent by the voids in the joint. Stress concentrations along the borders of microelements are common reasons for the decreased strength of brittle structures [21]. With a ductile bonding material such as Au, this effect should be reduced. The strength of a microbond might approach that of the metal itself in this case. Pure cast gold has a yield stress of about 125 MPa [22], but with the microstructure shown in Fig. 15, a hardening effect is to be expected. With small impurities precipitated in the Au grains, as the small strain contrast in the TEM micrograph of Fig. 10 might imply, a further hardening is obtained.

The results of the present investigation indicate that strong microbonds can be achieved using a solidified gold–silicon eutectic melt as an adhesive. For gold film thicknesses of 240 nm (substrate) and 200 nm (microblock), and an annealing temperature of 520 °C, bond strengths in the range 25–100 MPa were obtained. These values are as high as, or higher than, typical strength values of Si–glass anodically bonded microstructures [21] or Si–Si fusion bonds [5]. It has also been demonstrated for the first time that three-dimensional microassembly by means of eutectic bonding of micromachined elements can be performed by manipulation and processing on a locally heated specimen table.

Acknowledgements

The financial support of the Swedish Research Council for Engineering Science (TFR) for this project is gratefully acknowledged.

References

[1] H. Morishita and Y. Hatamura, Development of ultra precise manipulator system for future nanotechnology, *Proc. 1st Workshop Micro Robotics and Systems, Karlsruhe, Germany, 1993*, pp. 34–42.

[2] T. Sato, K. Koyano, M. Nakao and Y. Hatamura, Micro handling robot for micromachine assembly, *Proc. 1st Workshop Micro Robotics and Systems, Karlsruhe, Germany, 1993*, pp. 138–146.

[3] S. Johansson, Hybrid techniques in microrobotics, *Proc. 1st Workshop Micro Robotics and Systems, Karlsruhe, Germany, 1993*, pp. 72–83.

[4] J.B. Lasky, S.R. Stiffler, F.R. White and J.R. Abernathey, Silicon-on-insulator (SOI) by bonding and etch-back, *Proc. IEDM 1985, New York, 1985*, pp. 684–687.

[5] M. Shimbo, K. Furukawa, K. Fukuda and K. Tanzawa, Silicon-to-silicon direct bonding method, *J. Appl. Phys., 60* (1986) 2987–2989.

[6] L. Tenerz and B. Hök, Silicon microcavities fabricated with a new technique, *Electron. Lett., 22* (1986) 615–616.

[7] G. Wallis and D.I. Pomerantz, Field assisted glass–metal sealing, *J. Appl. Phys., 40* (1969) 3946–3949.

[8] A. Hanneborg, M. Nese and P. Øhlkers, Silicon-to-silicon anodic bonding with a borosilicate glass layer, *J. Micromech. Microeng., 1* (1991) 139–144.

[9] L.A. Field and R.S. Muller, Fusing silicon wafers with low melting temperature glass, *Sensors and Actuators, A21–A23* (1990) 935–938.

[10] J. Tirén, K.E. Bohlin and G. Alestig, Investigations of wafer bonding with BSPG surfaces, *Proc. Electrochem. Soc. Fall Meet., Phoenix, AZ, USA, 1991*, p. 695.

[11] L. Valero, The fundamentals of eutectic die attach, *Semiconductor Int., 7* (1984) 236–241.

[12] L.G. Feinstein, in *Electronics Materials Handbook*, ASM International, Materials Park, OH, USA, 1989, pp. 213–215.

[13] K.E. Bean, Anisotropic etching of silicon, *IEEE Trans. Electron Devices, ED-25* (1978) 1185–1192.

[14] D.L. Kendall and G.R. d. Guel, in C.D. Fung, P.W. Cheung, W.H. Ko and D.G. Fleming (eds.), *Micromachining and Micropackaging of Transducers*, Elsevier, Amsterdam, 1985, pp. 107–124.

[15] P.-H. Chang, G. Berman and C.C. Chen, Transmission electron microscopy of gold–silicon interactions on the backside of wafers, *J. Appl. Phys., 63* (1988) 1473–1477.

[16] F.Y. Shiau, H.C. Chang and L.J. Chen, Localized epitaxial growth of $CrSi_2$ on silicon, *J. Appl. Phys., 59* (1986) 2784–2787.

[17] N.P. Mencinger, M.P. Carthy and R.C. McDonald, Use of wetting angle measurements in reliability evaluations of Au–Si eutectic die attach, *Proc. Int. Reliability Physics Symp., Orlando, FL, USA, 1985, pp. 173–179.*

[18] H. Okamoto and T.B. Massalski, in T.B. Massalski (ed.), *Binary Alloy Phase Diagrams*, Vol. 1, ASM, Metals Park, OH, 1986, pp. 312–313.

[19] E. Philofsky, K.V. Ravi, J. Brooks and E. Hall, Phase transformations in eutectic gold–silicon alloys on single-crystal silicon, *J. Electrochem.: Solid-State Science Technol., 119* (1972) 527–530.

[20] W.A. Tiller, in R.W. Cahn (ed.), *Physical Metallurgy*, North-Holland, Amsterdam, 1974, pp. 437–442.

[21] S. Johansson, K. Gustafsson and J.-Å. Schweitz, Influence of bonded area ratio on the strength of FAB seals between silicon microstructures and glass, *Sensors Mater., 4* (1988) 209–221.

[22] J.A. Bard, in *Metals Handbook*, Vol. 2, ASM, Metals Park, OH, 1979, pp. 680–686.

Biographies

Anna-Lisa Tiensuu received her M.Sc. degree in engineering physics from Uppsala University in 1991. Since then she has been a Ph.D. student within the Micromechanics Programme at the Division of Materials Science, Uppsala University. Her research interests are material issues concerning bonding and microassembly techniques for microrobotics.

Mats Bexell received his M.Sc. degree in materials science from Uppsala University in 1992. Currently he is a Ph.D. student within the Micromechanics Programme at the Division of Materials Science, Uppsala University. His research interests are materials for microactuation intended for microrobotics.

Jan-Åke Schweitz received his B.Sc. degree in 1967 from the University of Gothenburg, and an M.Sc. degree in engineering physics from Uppsala University in 1969. He joined the Solid State Physics Department at the same university as a graduate student in 1970, and received his Dr.Sc. degree in 1975. In 1977 he became an associate professor, and since 1981 he has been acting as a full professor of materials science at Uppsala University. In 1984 he was one of the initiators of the Micromechanics Progamme in Uppsala, which is presently headed jointly by the two initiators.

Leif Smith received his M.Sc. degree in engineering physics in 1989 and his Ph.D. degree in 1993 at Uppsala University. Currently he is working at Radi Medical Systems AB, in Uppsala. His main research interests are micromachining for medical and fluidic systems.

Stefan Johansson was born in Avesta, Sweden in 1960. He received his M.Sc. degree in engineering physics in 1982 from Uppsala University. In 1983 he joined the Division of Materials Science, Uppsala University, where he was concerned with the development of methods for evaluation of the micromechanical properties of silicon. In 1988 he received his Dr.Sc. degree in materials science at Uppsala University. Since 1988 he has been working with different materials-science aspects of micromechanics, and in particular with the development of processing and design of microrobotics components. He holds a senior research position within the Micromechanics Programme at Uppsala University.